SUPPLEMENTARY MATERIALS AND METHODS

Cell lines and culture conditions

The cell lines used are detailed in **Supplemental Table 1**. Cells were purchased from the American Tissue Culture Collection (ATCC, Manassas, VA, USA). CD19 knock-out ($CD19^{KO}$), $CD22^{KO}$ and $CD19^{KO}/22^{KO}$ SEM cells were generated by CRISPR-mediated genome editing as detailed elsewhere(1). Suspension cell lines were maintained in RPMI-1640 supplemented with 2 mM L-glutamine, 10% heat-inactivated fetal bovine serum (FBS) and antibiotics (penicillin 100 units/mL, streptomycin 100 µg/mL). Adherent cell lines were grown in Dulbecco's Modified Eagle's Medium (DMEM) supplemented with 2 mM L-glutamine, 10% heat-inactivated FBS and antibiotics.

Vector construction

pCCL-CD22-4-1BB-CD3z-T2A-EGFP (CD22-CAR), pCCL-CD19-OKT3-His-T2A-tdTO (CD19-TCE) and pCCL-CD22-CD19-4-1BB-CD3z-T2A-EGFP (CD22-CD19-TanCAR) lentiviral vectors have been previously described(1-3). The pCCL-CD22-4-1BB-CD3z-F2A-CD19-OKT3-His-T2A-EGFP (CD22-CAR-CD19-TCE) was generated as follows. First, a synthetic gene encoding the F2A-CD19-TCE, flanked by *SgrA*I and *BstB*I, was synthesized by GeneArt AG (ThermoFisher Scientific, Regensburg, Germany) and subcloned into the pCCL-CD19-CAR vector(4), obtaining the pCCL-CD19-4-1BB-CD3z-F2A-CD19-OKT3-His plasmid. Then, the anti-CD19 scFv was swapped by the anti-CD22 scFv (clone hCD22.7) from CD22-CAR as *Mlu*I/*Mre*I, to create the pCCL-CD22-CAR-F2A-CD19-TCE vector. The last step involved the addition of the EGFP in C-terminal position, following a T2A cleavage sequence, as *AfeI*/*BstB*I, to obtain the final pCCL-CD22-CAR-F2A-CD19-TCE-T2A-EGFP vector (CD22-CAR-CD19-TCE).

Arroyo-Ródenas J, *et al. J Immunother Cancer* 2025; 13:e009048. doi: 10.1136/jitc-2024-009048

Lentiviral vector production and titration

To produce third-generation lentiviral particles, HEK293T cells were transfected with vectors encoding the sequence of interest together with the packaging plasmids pMDLg/pRRE and pRSVrev and the envelope plasmid pMD2.G (all from Plasmid Factory, Bielefeld, Nordrhein-Westfalen, Germany), using polyethyleneimine (PEI) of 25 kDa molecular weight (Polysciences, Warrington, PA, USA). After 48 hours, viral supernatants were collected, clarified by centrifugation, and ultracentrifuged for 2 hours at 26,000 rpm. Pellets containing the lentiviral vectors were resuspended in Phosphate Buffered Saline (PBS), aliquoted and stored at −80 °C until use. Functional titers of CD22-CAR-, CD19-TCE-, CD19-CD22-TanCAR- and CD22-CAR-CD19-TCE-encoding lentiviruses were determined by limiting dilution in Jurkat cells and analyzed using EGFP expression by flow cytometry. Viral titers were consistently in the range of 5x107-5x108 infection units (IFUs)/mL.

Enzyme-linked immunosorbent assays (ELISA)

Antibodies used in ELISA assays are detailed in **Supplemental Table 2**. To detect the CD19-TCE secreted to culture supernatants, recombinant human CD19 Fc chimera (hCD19-Fc, R&D Systems) was immobilized (5 mg/mL) on Maxisorp 96-well plates (NUNC) overnight at 4ºC. After washing and blocking, conditioned media was added and incubated for 1 hour at room temperature (RT). Then, wells were washed 3 times with PBS-0.05% Tween20 and 3 times with PBS and incubated for 1 hour with anti-His mAb (Qiagen, 1 mg/mL). Finally, after washing, the plate was developed using 100 µl of 3,3′,5,5′-tetramethylbenzidine (TMB) (Sigma-Aldrich) and stopped by 100 µl of 1N H_2SO_4. Absorbance was read at 450 using Multiskan FC photometer (Thermo Scientific). Concentrations of the T Cell Engager (TCE) were interpolated from a standard curve of blinatumomab (Amgen Inc, Thousand Oaks, California). IFNγ secretion was analyzed by ELISA using a commercial kit (Diaclon).

Western blotting

Antibodies used in Western blotting assays are detailed in **Supplemental Table 2.** Samples were separated under reducing conditions on 10%–20% Tris-glycine gels (Life Technologies, Paisley, UK), transferred onto PVDF membranes (Merck Millipore, Tullagreen, Carrigtwohill, Ireland) and probed with 200ng/mL anti-poly Histidine (His) mAb (Qiagen, Hilden, Germany), followed by incubation with 1.6µg/mL horseradish peroxidase (HRP)-conjugated goat anti-mouse (GAM) IgG, Fc specific (Sigma-Aldrich, St. Louis, MO, USA). Visualization of protein bands was performed with Pierce™ ECL Western Blotting substrate (ThermoFisher) and ChemiDoc MP Imaging System machine (Bio-Rad Laboratories, Hercules, CA, USA).

Flow cytometry

Antibodies used for flow cytometry analysis are detailed in **Supplemental Table 3**. DAPI (Sigma-Aldrich) and 7-Aminoactinomycin D (7-AAD; BD Biosciences) were used as viability markers. Cell surface expression of CD22-CAR was analyzed by incubation with recombinant human CD22 Fc Chimera Protein (hCD22-Fc; R&D Systems, Minneapolis, MN, USA) followed incubation with a Brilliant Violet (BV421)-conjugated anti-human IgG-Fc specific antibody (Biolegend, San Diego, CA, USA). Intracellular expression of CD19-TCE was assessed using an APC-conjugated anti-His mAb (Miltenyi Biotec) and the Inside Stain Kit (Miltenyi Biotec), following manufacturer's instructions. Alternatively, the expression of CD22-CAR and CD19-TCE was estimated based on EGFP fluorescent protein expression. Cell acquisition was performed in a DxFlex flow cytometer using CytExpert software (Beckman Coulter, Brea, CA, USA). Analysis was performed using FlowJo V10 (FlowJo LLC, Ashland, OR, USA) or Kaluza V2.3 (Beckman Coulter) software.

Immunofluorescence and confocal microscopy

Jurkat effector T cells (J-NT-T, J-CAR-22T, J-STAb-19T, J-TanCAR-T or J-CAR-STAb-T) were incubated at 37 °C for 15 minutes with Raji target cells at a 1:1 E:T ratio. Co-cultures of 1.5 x 10^5 J-NT-T cells and 1.5 x 10^5 Raji Superantigen E (SEE)-loaded cells (pre-incubated with CMAC 1 μM) were used as a positive control for immune synapse assembly. Jurkat/Raji conjugates (1.5 x 10^5 cells each) were fixed with 4% paraformaldehyde (Sigma-Aldrich) in PBS for 5 minutes at room temperature and permeabilized (5 minutes at room temperature) with 0.1% Triton X-100 (Sigma-Aldrich) during 5 minutes at room temperature. Samples were then blocked with 10 μg/mL human γ-globulin for 20 minutes at room temperature and stained with the antibodies listed in **Supplemental Table 4** for 1 hour at room temperature. Then, cells were washed with TBS (Tris 20 mM, NaCl 150 mM) and incubated with Alexa Fluor™ 488 or 594 α-rabbit secondary antibody and phalloidin-Alexa Fluor™ 647 at room temperature for 30 minutes. Coverslips were washed twice with TBS and once with distilled water before being mounted with Mowiol medium. Confocal sections of fixed samples were acquired using a Leica SP-8 confocal scanning laser microscopy with a 60X/1.35 oil immersion objective. Alexa Fluor™ 488, Alexa Fluor™ 594 and phalloidin-Alexa Fluor™ 647 were excited with 488, 594 and 633 nm laser lines, respectively. Image acquisition was automatically optimized with the Leica SP-8 confocal scanning laser microscopy software (Leica Mycrosystems) to get an image resolution of 58 nm/pixel. Analysis of images was conducted with ImageJ freeware (National Institutes of Health). The polarization of CD3ε at the immunological synapse (IS) was estimated with the Synapse Measure plugin(5). Actin clearance was calculated as the ratio between the central actin cleared area and the total area of the interface obtained from the 3D reconstruction of each individual synapse.

Cell-trace-stained tumor escape assays

To assess CD19 and CD22 expression dynamics in leukemia cells that escape tumor control *in vitro*, 3 x 10^6 SEM WT, $CD19^{KO}$ or $CD22^{KO}$ cells were stained at day 0 for 20 min at 37 ºC with the following CellTrace™ dyes (ThermoFischer):

Cell line	CellTrace™	Reference	Concentration
SEM^{WT}	Far Red	C34572	0.1 uM
SEM-$CD19^{KO}$	Violet	C34571	0.5 uM
SEM-$CD22^{KO}$	CFSE	C34570	0.5 uM

The staining reaction was stopped with FBS at 4 ºC for 5 min and cells were washed twice in PBS before setting the co-cultures with primary transduced T cells.

Multiplex bead-based immunoassays

Cytokine secretion from *in vitro* supernatants (IFN-γ, IL-2 and Granzyme B) and *in vivo* plasma and CSF samples (IFN-γ, IFN-β, IL-1β, IL-6 and IL-10) was measured in multiplex bead-based immunoassays (ProcartaPlex, ThermoFischer) and developed using LABScan3D multiplex flow analyzer (One lambda, Canoga Park, LA, USA).

SUPPLEMENTARY FIGURES

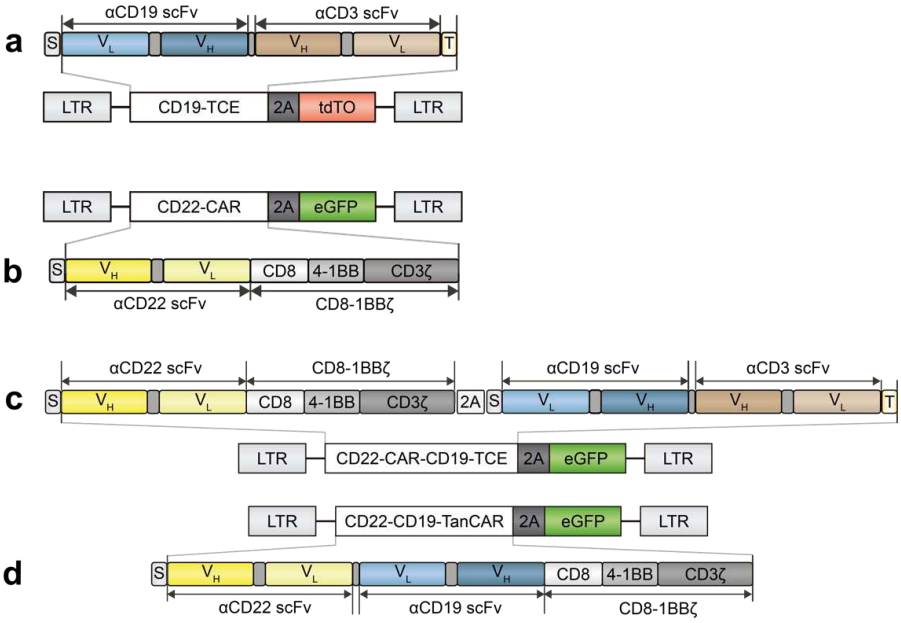

Figure S1. Schematic diagrams of CD19-TCE, CD22-CAR, CAR-STAb and TanCAR constructs. (a-d) Schematic diagrams showing the genetic structure of (a) CD19-TCE, bearing signal peptide from the human k light chain (S, grey box), the anti-CD19 (A3B1) scFv gene (blue boxes), the anti-CD3 OKT3 scFv gene (brown boxes) and His tag (light yellow box); (b) CD22-CAR, bearing the CD8a signal peptide (S, gray box), the CD22 (hCD22.7) scFv gene (yellow boxes), followed by the human CD8 transmembrane domain and the human 4-1BB and CD3ζ endodomains (gray); (c) CAR-22-STAb-19 structure, containing CD22-CAR (Fig S1b) and CD19-TCE (Fig S1a) cassettes, separated by a F2A sequence; and (d) CD19-CD22 TanCAR construct, containing anti-CD19 (A3B1) scFv in the more proximal location of the construct, separated from the more distal CD22 scFv by a short $(G_4S)_4$ linker. All constructs were cloned into a pCCL lentiviral-based backbone containing a T2A-reporter gene (either GFP or tdTO) cassette.

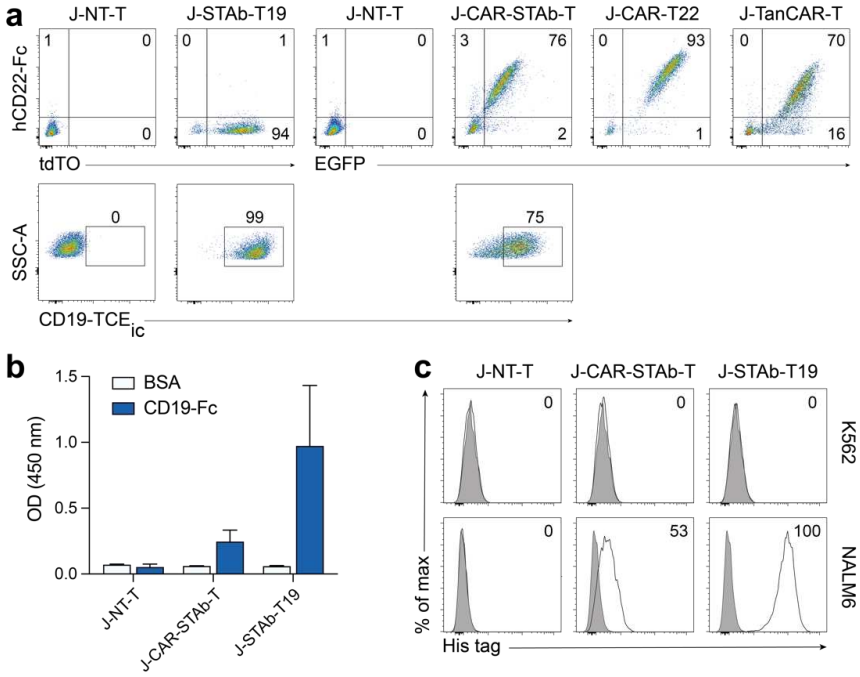

Figure S2. Characterization of transduced cells and analysis of CD19-TCE secretion and binding capacity in a Jurkat cell model. (a) Transduction efficacy in Jurkat cells calculated by CD22-CAR surface expression or intracellular CD19-TCE, detected with purified human CD22-Fc chimera or anti-poly Histidine (His), respectively. Due to a good correlation between these values and reporter protein expression, transduction efficacy was also estimated by the percentage of EGFP/tdTO-positive cells. A representative transduction of three is shown (*n*=3). (b) Detection of soluble functional CD19-TCE in the conditioned media from J-NT-T, J-STAb-T and J-CAR-STAb-T cells by ELISA against plastic-immobilized human CD19-Fc chimera (hCD19) or BSA. Data expressed as mean ± standard error of mean (SEM) of two independent experiments (*n*=2). (c) Specific binding capacity of the CD19-TCE, secreted by J-CAR-STAb-T and J-STAb-T cells, to NALM6 or K562 cells was demonstrated by flow cytometry. Histograms shown correspond to one representative of three independent experiments (*n*=3).

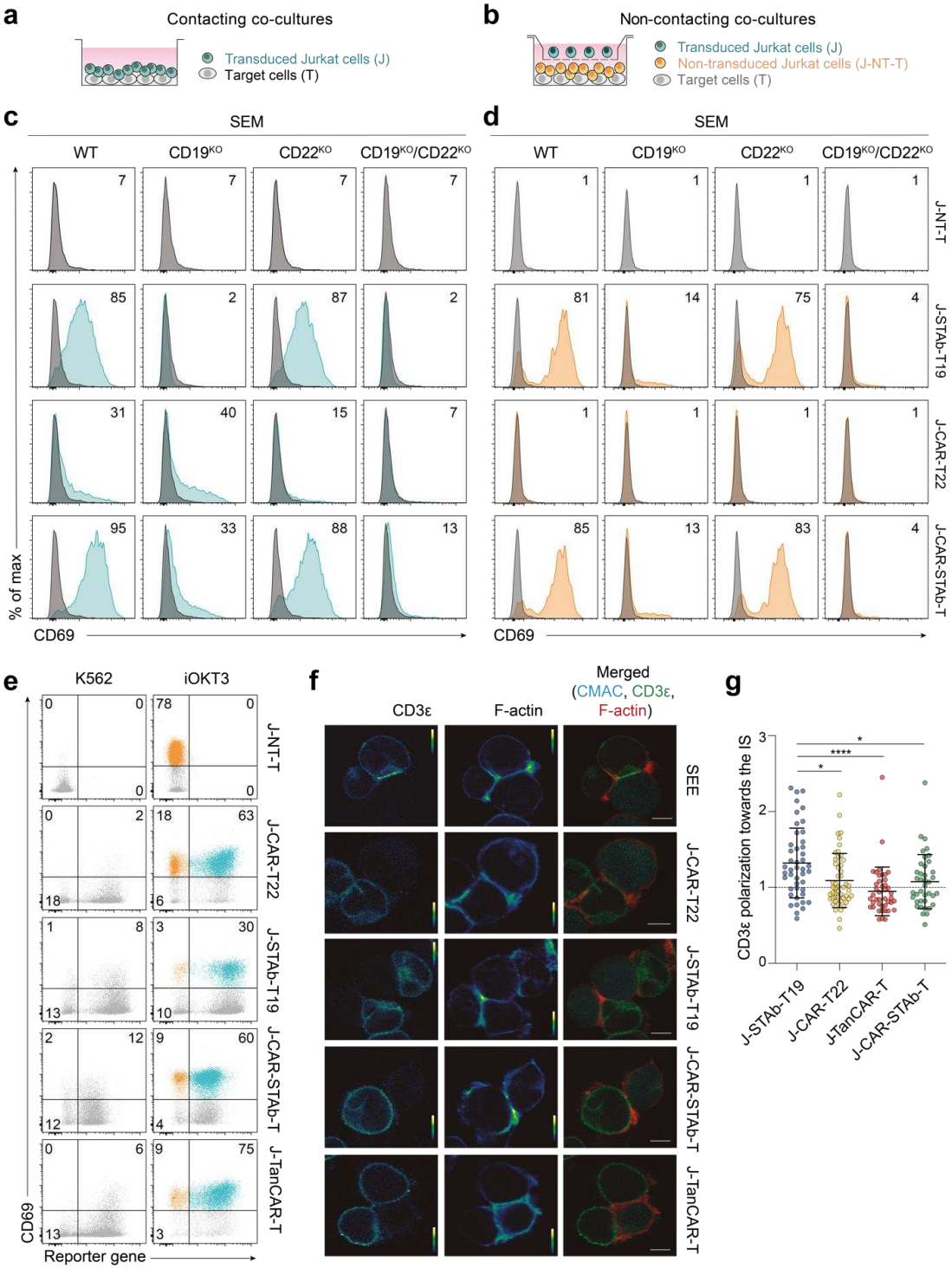

Figure S3. CAR-STAb-T Jurkat cells mediate specific activation and immunological synapse formation when co-culture with CD19- and/or CD22-positive target cells. (a,b) Schematic representation of direct contact (a) or transwell (b) co-culture systems to study

Arroyo-Ródenas J, *et al. J Immunother Cancer* 2025; 13:e009048. doi: 10.1136/jitc-2024-009048

specific activation of J-NT-T, J-STAb-T19, J-CAR-T22 and J-CAR-STAb-T cells against a panel of SEM cells genetically engineered using CRISPR-Cas9 technology to selectively silence the expression of one and/or two of the target antigens. (c, d) T cell activation after 24 hours was measured by flow cytometry. Percentages of CD69-positive cells are indicated. (e) Activation of transduced (teal) and non-transduced (orange) Jurkat cells cultured with K562 cells (negative control) or in a pre-coated plate with 1 ug/mL of anti-CD3 (OKT3) monoclonal antibody (positive control). One of three independent experiments measuring CD69 by flow cytometry is shown (n=3). Percentages of activated ($CD69^{pos}$) Jurkat cells are indicated. (f,g) CD3ε polarization towards the IS induced by J-STAb-T19, J-CAR-T22, J-TanCAR-T and J-CAR-STAb-T cells. (f) Conjugates of Jurkat and SEE-loaded Raji cells are used to show actin organization of canonical IS. CD3ε and F-actin distribution to the IS of a confocal section is displayed in pseudo color. The calibration bar of the pseudo color is indicated. The right column of images illustrates the distribution of merged CD3ε (green), F-actin (red) and CMAC (cyan). Scale bar corresponds to 5 µm. Representative Jurkat/Raji cell conjugates are shown. (g) Graph projects the polarization of CD3ε to the IS. Each dot represents the value of individual cell interactions obtained from n=2 independent experiments. The dashed line represents a CD3ε polarization ratio cut-off of 1. Statistical significance was calculated by one-way ANOVA test corrected with a Tukey's multiple comparison test.

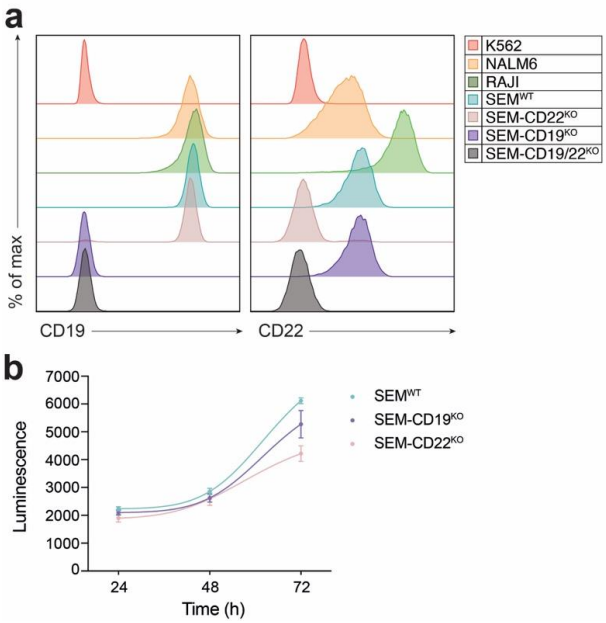

Figure S4. Cell line characterization. (a) CD19 and CD22 surface expression in K562, NALM6, Raji and the SEM cell line panel. (b) Proliferation dynamics of SEM^{WT}, SEM-CD22^{KO} and SEM-CD19^{KO} cells after 72 hours in culture. Data expressed as mean ± SEM of three triplicates from one experiment (*n*=3).

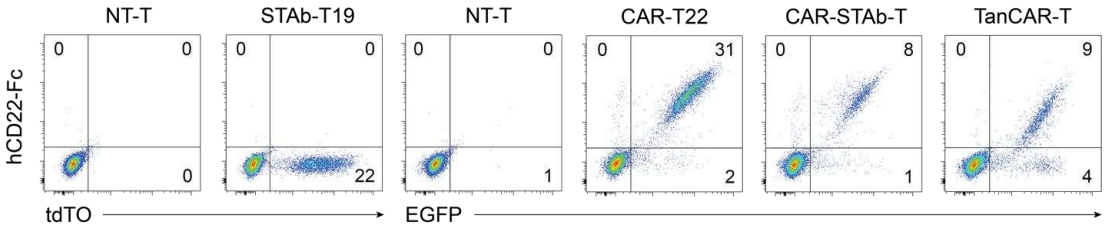

Figure S5. Transduction efficiency in human primary T cells. Reporter gene (tdTO or EGFP) and CD22-CAR surface expression detected with human CD22-Fc chimera (hCD22-Fc) and anti-Fc antibody by flow cytometry. One representative transduction of at least three performed is shown (*n*=3). Numbers represent the percentage of cells staining positive for the indicated marker.

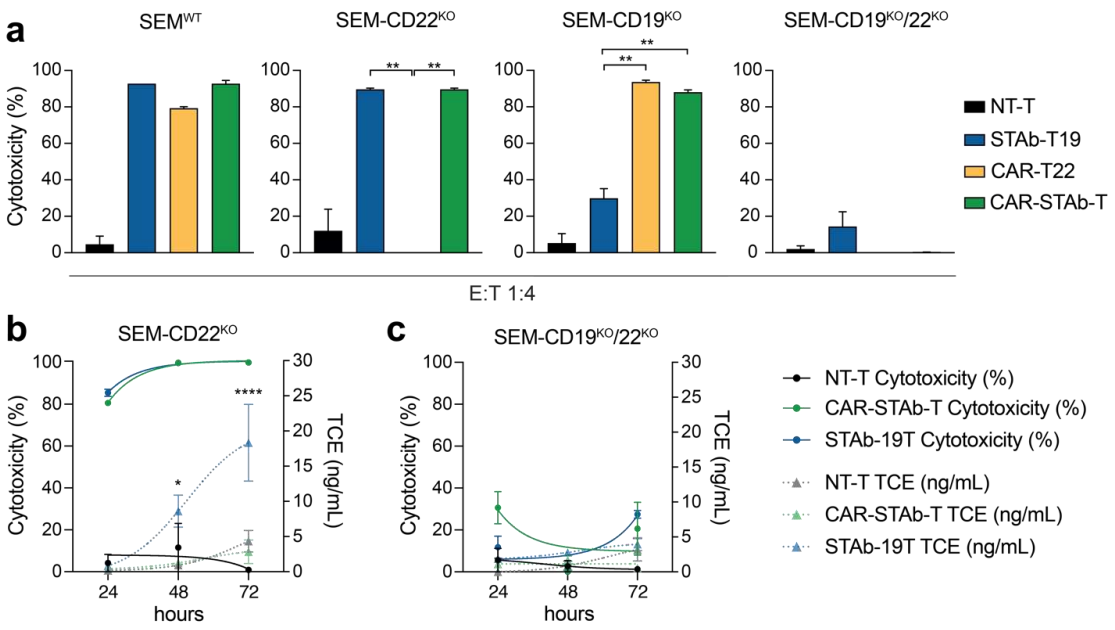

Figure S6. Specific cytotoxic activity and TCE secretion mediated by CAR-T22, STAb-T19 and CAR-STAb-T cells. (a) NT-T, CAR-T22, STAb-T19 or CAR-STAb-T cells were co-cultured with the SEM cell panel described in Figure S3 at 1:4 E:T ratio. After 48 hours, the percentage of specific cytotoxicity was calculated by addition of D-luciferin to detect bioluminescence. Data expressed as mean ± SEM of one experiment in duplicate (*n*=2). (b-c) NT-T, STAb-T19 or CAR-STAb-T cells were co-cultured with SEM-CD22^{KO} (b) or SEM-CD19^{KO}/22^{KO} (c) target cells at 1:1 E:T ratio. Cytotoxicity (left axis) and TCE secretion (right axis) were measured at 24, 48 and 72 hours by bioluminescence and ELISA, respectively. Data expressed as mean ± SEM of one experiment in triplicate (*n*=3). Statistical significance was calculated by two-way ANOVA test corrected with a Tukey's multiple comparisons test.

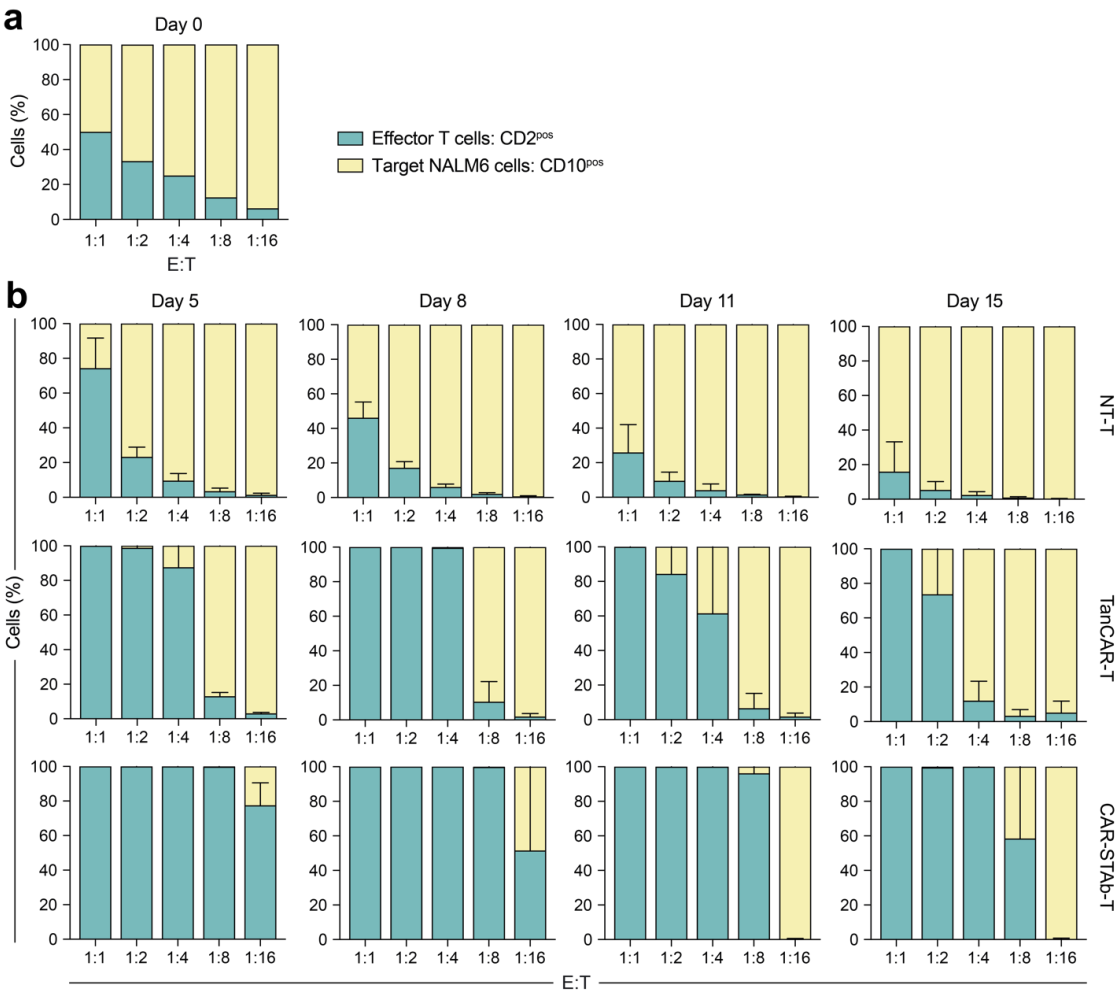

Figure S7. CAR-STAb-T cells prevent escape of CD19^{pos}/CD22^{pos} tumor cells *in vitro* more efficiently than TanCAR-T cells. Leukemia escape from immune pressure. (a) NALM6^{Luc} cells were co-cultured with NT-T, CAR-STAb-T or TanCAR-T cells at the indicated E:T ratios and the expression of CD2 and CD10 was analyzed after 5, 8, 11 and 15 days by flow cytometry. (b) Graphs show the change over time in relative percentages of CD2^{pos} CD10^{neg} and CD2^{neg} CD10^{pos} cells. Data expressed as mean ± SEM of two experiments with independent donors (*n*=2).

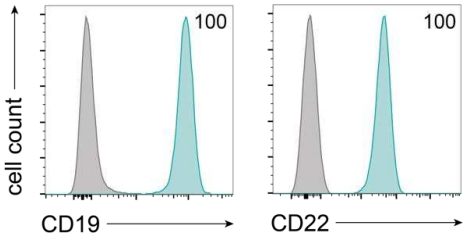

Figure S8. CD19 and CD22 expression in human primary B-ALL patient-derived xenograft. CD19 and CD22 surface expression by flow cytometry on human B-ALL PDX injected to NSG mice. Tumor cells were gated as HLA-ABC^{pos}, CD3^{neg} cells.

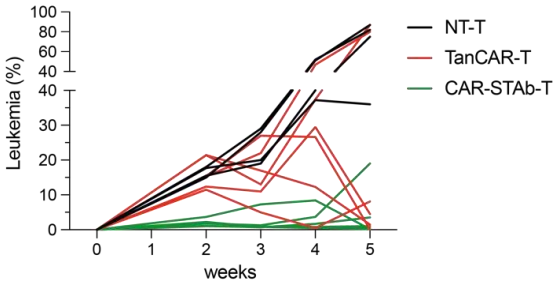

Figure S9. Comparative *in vivo* efficacy of CAR-STAb-T and TanCAR-T cells in tumor models co-expressing CD19 and CD22. Percentage of leukemic cells measured by flow cytometry in peripheral blood. Each line represents an independent mouse (n=4 for NT-T group and n=6 for CAR-STAb-T and TanCAR-T groups).

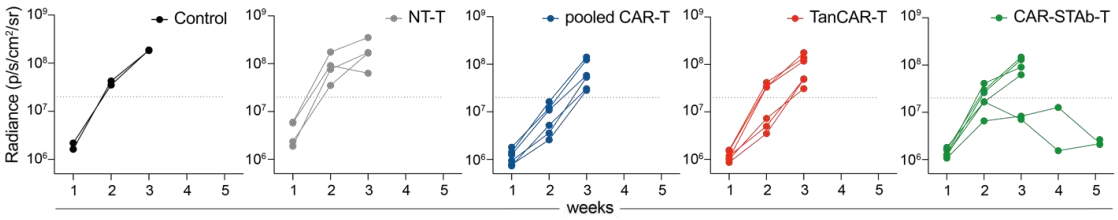

Figure S10. Comparative *in vivo* efficacy and tumor escape in a tumor model with heterogenous expression of CD19 and CD22. Radiance quantification (photons s−1 cm−2 sr−1) for the different groups at the indicated time points. A humane endpoint of 2 x 10^7 photons s−1 cm−2 sr−1 was established. Each line represents an individual mouse (2 mice for control

Arroyo-Ródenas J, *et al. J Immunother Cancer* 2025; 13:e009048. doi: 10.1136/jitc-2024-009048

group, 4 mice for NT-T group and 6 mice for CAR-STAb-T, TanCAR-T and pooled CAR-T groups).

Arroyo-Ródenas J, *et al. J Immunother Cancer* 2025; 13:e009048. doi: 10.1136/jitc-2024-009048

SUPPLEMENTARY TABLES

Table S1. Cell lines.

SUSPENSION	
Name	**ATCC code**
Jurkat (E6-1)	TIB-152
NALM6 (G5)	CRL3273
SEM	CVCL_0095*
Raji	CCL-86
K562	CCL-243

ADHERENT	
Name	**ATCC code**
HEK293T	CRL-3216

*https://www.cellosaurus.org/CVCL_0095

Table S2. Antibodies used in ELISA and Western blotting assays.

MONOCLONAL ANTIBODIES				
Target	**Conjugation**	**Clone**	**Supplier**	**Catalog number**
Penta-His	-		Qiagen[1]	34660

POLYCLONAL ANTIBODIES				
Target	**Conjugation**		**Supplier**	**Catalog number**
Goat anti-mouse IgG	HRP	-	Sigma-Aldrich[2]	A2554
Goat anti-mouse IgG	HRP	-	Jackson Immuno Research[3]	115-035-166

1 Qiagen, Hilden, Germany
2 Sigma-Aldrich, San Luis, MO, USA
3 Jackson ImmunoResearch, West Grove, PA, USA

Table S3. Antibodies used in flow cytometry assays.

MONOCLONAL ANTIBODIES				
Target	**Conjugation**	**Clone**	**Supplier**	**Catalog number**
human CD2	V450	S5.2	BD Biosciences[1]	644485
human CD3	PB	UCHT1	Beckman Coulter[2]	B49204
human CD3	PerCP-Cy5.5	UCHT1	Beckman Coulter[2]	B49203
human CD4	APC	RPA-T4	BD Biosciences	555349

human CD8	APC-Cy7	SK1	Biolegend[3]	344714
human CD10	APC	HI10a	BD Biosciences	340923
human CD19	PC5	J3.119	Beckman Coulter	A66328
human CD19	PC7	J3.119	Beckman Coulter	IM3628
human CD19	Brilliant Violet 421	HIB19	BD Biosciences	562440
human CD22	APC	HIB22	BD Biosciences	562860
human CD22	BV605	HIB22	BD Biosciences	740396
human CD69	PE-Cy7	L78	BD Biosciences	335792
human CD69	APC	L78	BD Biosciences	340560
human CD45	Brilliant Violet 510	HI30	BD Biosciences	563204
human CD45RA	V500	HI100	BD Biosciences	561640
human CCR7	BV421	150503	BD Biosciences	562555
HLA-ABC	PE	G46-2.6	BD Biosciences	555553
His	APC	GC11-8F3.5.1	Miltenyi Biotec[4]	130-119-782
Rat anti-human IgG Fc	Brilliant Violet 421	M1310G05	Biolegend[5]	409317

1 BD Biosciences, San Jose, CA, USA
2 Beckman Coulter, Marseille Cedex, France
3 Biolegend, San Diego, CA, USA
4 Miltenyi Biotec, Bergisch Gladbach, Germany
5 Biolegend, San Diego, CA, USA

Table S4. Antibodies used in immunofluorescence and confocal microscopy assays.

MONOCLONAL ANTIBODIES				
Target	**Conjugation**	**Clone**	**Supplier**	**Catalog number**
CD3ε	-	T3b	F. Sánchez-Madrid[1]	-

POLYCLONAL ANTIBODIES				
Target	**Conjugation**		**Supplier**	**Catalog number**
Goat anti-mouse IgG	Alexa Fluor 488	-	Thermo Fischer Scientific[2]	A-11001
Goat anti-mouse IgG	Alexa Fluor 594	-	Thermo Fischer Scientific[2]	A-11032

PROBES AND MARKERS				
Target	**Conjugation**		**Supplier**	**Catalog number**
Phalloidin	Alexa Fluor 647	-	Thermo Fischer Scientific[2]	A22287
CellTracker™ Blue CMAC	-	-	Thermo Fischer Scientific[2]	C2110

1 Dr. Francisco Sánchez-Madrid, Hospital Universitario de la Princesa, Madrid, Spain
2 Thermo Fischer Scientific, MA, USA.

1. Zanetti SR, Velasco-Hernandez T, Gutierrez-Agüera F, Díaz VM, Romecín PA, Roca-Ho H, et al. A novel and efficient tandem CD19- and CD22-directed CAR for B cell ALL. Mol Ther. 2022;30(2):550-63.
2. Blanco B, Ramírez-Fernández Á, Bueno C, Argemí-Muntadas L, Fuentes P, Aguilar-Sopeña Ó, et al. Overcoming CAR-Mediated CD19 Downmodulation and Leukemia Relapse with T Lymphocytes Secreting Anti-CD19 T-cell Engagers. Cancer Immunol Res. 2022;10(4):498-511.
3. Velasco-Hernandez T, Zanetti SR, Roca-Ho H, Gutierrez-Aguera F, Petazzi P, Sánchez-Martínez D, et al. Efficient elimination of primary B-ALL cells in vitro and in vivo using a novel 4-1BB-based CAR targeting a membrane-distal CD22 epitope. J Immunother Cancer. 2020;8(2).
4. Castella M, Boronat A, Martín-Ibáñez R, Rodríguez V, Suñé G, Caballero M, et al. Development of a Novel Anti-CD19 Chimeric Antigen Receptor: A Paradigm for an Affordable CAR T Cell Production at Academic Institutions. Mol Ther Methods Clin Dev. 2019;12:134-44.
5. Calabia-Linares C, Robles-Valero J, de la Fuente H, Perez-Martinez M, Martín-Cofreces N, Alfonso-Pérez M, et al. Endosomal clathrin drives actin accumulation at the immunological synapse. J Cell Sci. 2011;124(Pt 5):820-30.